RESULTS AND DISCUSSION

Part A: Gaussian Calculations

1. Conformational and Structural Analysis

The conformational analysis of 2-pyridine-(9,9'-diethylfluorene) (EFPy) monomer was calculated at the semi-empirical (AM1), *ab initio* (HF/3-21G, HF/3-21G*, HF/6-31G, HF/6-31G*, HF/6-31G**) and density functional theory (B3LYP/6-31G and B3LYP/6-31G*). The octyl groups at the 9 position have been replaced by ethyl groups to reduce the time of calculation. Figure 6 shows potential energy curves of EFPy monomer as the calculations were done by changing the torsional angle, (θ=C_{10}-C_{11}-C_{14}-C_{15}) by 15° steps from 0 to 360^{o}. The symmetry potential energy curves are obtained from 0 to 360^{o}. Therefore, potential energy curves of EFPy monomer from 0 to 180^{o} are shown in Figure 7. From Figure 7, *ab initio* and density functional theory methods give very similar potential energy curves with the same minima (0-30^{o} and 150-180^{o}) and similar potential barriers. Whereas, semiempirical method (AM1) reveals a different minima located around 30-45^{o} and 135-150^{o}. However, it was found that all calculations give nonplanar structures.

In following, the results show that basis set without polarization functions is not good enough to predict good potential energy curves. On the other hand, it is not necessary to apply double polarization functions. Therefore, using polarization seems essential and HF/3-21G* is the minimal basis set for determination of potential energy curves. The reason is that the results obtained from the HF/3-21G* method have been shown to give a very good correlation between the density functional theory with the 6-31G* basis set.

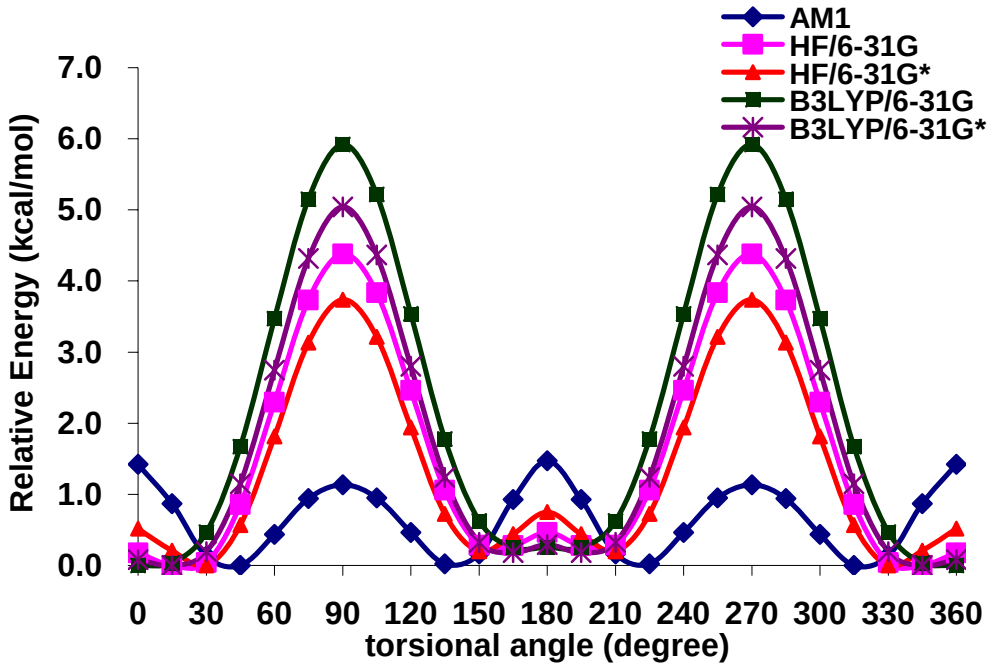

Figure 6 Ground state potential curves of EFPy monomer as obtained from AM1, HF/6-31G, HF/6-31G*, B3LYP/6-31G and B3LYP/6-31G* (θ = 0-360^{o}).

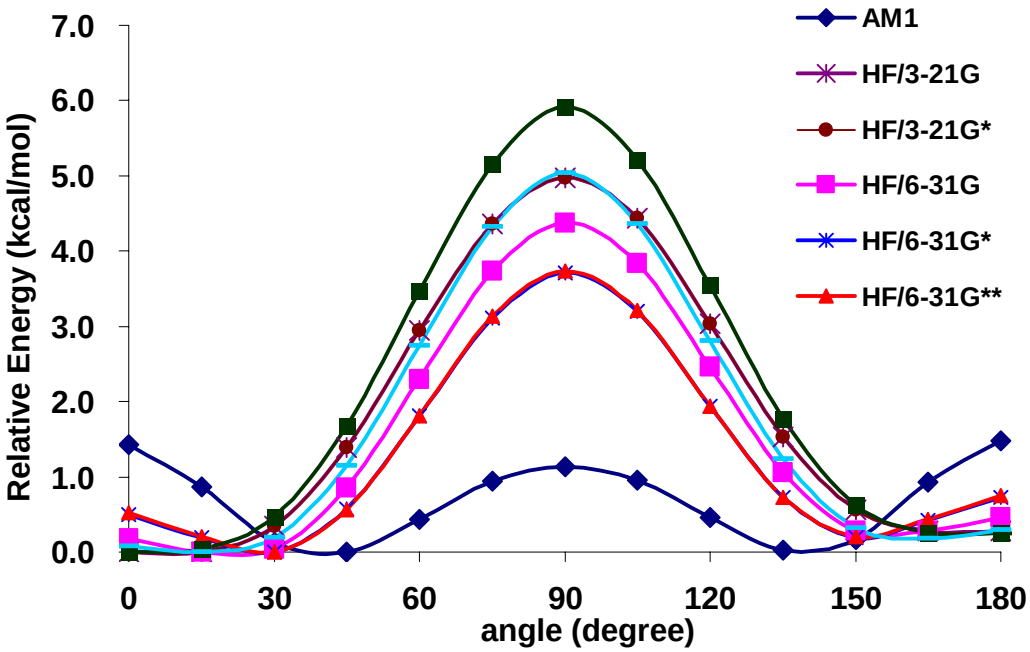

Figure 7 Ground state potential curves of EFPy monomer calculated at the AM1, HF/3-21G, HF/3-21G*, HF/6-31G, HF/6-31G*, HF/6-31G**, B3LYP/6-31G and B3LYP/6-31G* (θ = 0-180^{o}).

2. Ground State Geometries

Optimized ground state geometries of EFPy monomer obtained using AM1 semi-empirical, Hartree Fock with the 3-21G* and 6-31G* level of calculations and Density Functional Theory with the 6-31G* basis set were displayed in Table 2. According to Table 2, it was found that the bond distances obtained from AM1, HF/3-21G*, HF/6-31G* and B3LYP/6-31G* methods are not significantly difference, however the torsional angles between fluorene and pyridine units show a significant difference. Recently, the conformational analysis of fluorene derivatives has been studied using HF/6-31G* *ab-initio* calculations (Belletête *et al.*, 2000, Blondin *et al.,* 2000, Leclerc *et al.,* 2001, Tirapattur *et al.,* 2003 and Poolmee *et al.,* 2004). Comparing the optimized inter-ring distance (C_{10}-C_{14}) and torsional angle (C9-C10C-14-C19) of EFPy with bifluorene (FF) as obtained from HF/6-31G* level, we observed that the inter-ring distance of EFPy is very close to that obtained for FF using the same level of calculation (r = 1.491 Å, Blondin *et al.*, 2000). The torsional angle of EFPy is smaller than that of FF (torsional angle = 43.3°, Blondin *et al.,* 2000). As expected, the pyridine unit creates less steric hindrance than the fluorene ring.

In addition, the comparison of EFPy and fluorene-phenylene monomer (FP) at HF/6-31G* method of calculation, it was found that the torsional angle of EFPy as obtained at the HF/6-31G* is 28.5°. The torsional angle of EFPy is less twisted than that of FP (Fluorene-Phenylene monomer) (torsional angle = 45.3°) (Belletête *et al.,* 2000). This shows that the most stable conformer of EFPy is just slightly more planar than that of FP. Moreover, the EFPy showed the twisted torsional angle is less than that of FP due to the substitution of nitrogen atom on the phenyl ring. This can be explained by the combination of two factors: first, a less steric hindrance effect caused by nitrogen atom due to the smaller than the carbon atom. Second, a better-acceptor effect between

Table 2 Optimized geometry parameters of EFPy monomer; bond lengths (Å), bond angles (°) and torsional angles (°).

Bond length	EFPy							FP[a]	x-ray[b]
(Å)	AM1	HF/3-21G	HF/3-21G*	HF/6-31G	HF/6-31G*	B3LYP/6-31G	B3LYP/6-31G*	HF/6-31G*	
C1-C2	1.402	1.386	1.387	1.389	1.386	1.400	1.396	1.386	1.40
C2-C3	1.380	1.386	1.387	1.389	1.386	1.390	1.396	1.386	1.41
C3-C4	1.420	1.390	1.390	1.390	1.390	1.410	1.410	1.385	1.41
C4-C5	1.380	1.380	1.370	1.380	1.380	1.390	1.390	1.381	1.38
C5-C6	1.400	1.380	1.390	1.390	1.390	1.400	1.400	1.389	1.43
C6-C1	1.390	1.380	1.380	1.380	1.380	1.400	1.390	1.389	1.38
C7-C8	1.385	1.380	1.380	1.384	1.384	1.398	1.396	1.386	
C8-C9	1.390	1.380	1.380	1.384	1.384	1.398	1.396	1.384	
C9-C10	1.400	1.390	1.390	1.390	1.390	1.410	1.400	1.396	
C10-C11	1.400	1.390	1.390	1.390	1.390	1.410	1.410	1.395	
C11-C12	1.380	1.370	1.370	1.370	1.370	1.380	1.380	1.380	
C12-C7	1.420	1.390	1.390	1.390	1.390	1.410	1.410	1.394	
C10-C14	1.470	1.480	1.480	1.480	1.490	1.480	1.480	1.490	
C14-N15	1.360	1.330	1.330	1.390	1.320	1.400	1.350	1.394	
N15-C16	1.340	1.320	1.320	1.380	1.320	1.390	1.330	1.384	
C16-C17	1.400	1.380	1.380	1.380	1.380	1.400	1.390	1.386	
C17-C18	1.390	1.380	1.380	1.380	1.380	1.390	1.390	1.386	
C18-C19	1.390	1.380	1.380	1.320	1.380	1.340	1.390	1.384	
C19-C14	1.410	1.390	1.390	1.340	1.390	1.360	1.400	1.392	

Table 2 Optimized geometry parameters of EFPy monomer; bond lengths (Å), bond angle (°) and torsional angle (°) (cont'd).

Bond angle (°)	EFPy							FP[a]	x-ray[b]
	AM1	HF/6-31G*	HF/3-21G*	HF/6-31G	HF/6-31G*	B3LYP/6-31G	B3LYP/6-31G*		
C7-C8-C9	118.8	119.0	119.0	118.8	118.8	119.1	119.0		
C8-C9-C10	121.0	121.2	121.2	121.3	121.3	121.4	121.5		
C9-C10-C11	120.4	119.2	119.2	119.0	119.0	118.7	118.8		
C10-C11-C12	118.8	119.8	119.8	119.8	120.0	120.0	120.0		
C11-C12-C7	120.6	120.5	119.8	120.8	120.6	120.8	120.6		
C12-C7-C8	120.4	120.3	120.5	120.3	120.4	120.0	120.0		
C9-C10-C14	119.5	122.3	122.3	121.5	121.3	120.1	121.8		
C11-C10-C14	120.1	118.6	118.6	119.5	119.7	119.3	119.4		
C10-C14-C19	118.8	123.0	123.0	122.9	121.7	123.3	122.3		
C10-C14-N15	119.1	116.7	116.7	117.0	116.7	116.4	116.5		
C14-C19-C18	119.2	119.4	119.4	119.6	119.1	120.0	119.6		
C19-C18-C17	119.1	119.6	119.6	119.5	119.2	119.3	118.9		
C18-C17-C16	118.1	117.8	117.8	117.6	177.5	117.7	117.7		
C17-C16-N15	124.0	122.5	122.5	122.8	123.8	123.5	124.1		
C16-N15-C14	117.6	120.5	120.5	120.4	119.1	119.3	118.6		
N15-C14-C19	122.1	120.3	120.3	120.2	121.4	120.3	121.2		
C9-C10C-14-C19	40.2	-11.5	-11.5	-23.2	-28.5	-8.1	-18.6	45.3	

[a]Belletête *et al.*, 2000.

[b]Burns *et al.*, 1955.

fluorene and pyridine rings. In addition, in case of fluorene unit, the results obtained from AM1, *ab initio*, and DFT are in good agreement with the reported X-ray data (Burns *et al*., 1955).

The optimized bond distances, angles and torsional angles of Poly-2,5-pyridine-(9,9'-diethylfluorene) $(EFPy)_n$, n = 1-5 calculated from HF/6-31G* are shown in Table 3 and 4, respectively. It was found that the optimized geometry parameters of the oligomeric molecules change softly with increasing chain length in the series of polymer. Therefore, the basic structures of the polymer can be described as their oligomers. Additionally, all molecules indicate nonplanar structures. Figure 8 showed the optimized structure of $(EFPy)_n$, n = 1-5. Moreover, as the chain length increased, the large torsional angle occurred in the middle parts of molecule and much smaller near the ends.

Table 3 Optimized bond distances of $(EFPy)_n$ (n = 1-5) as obtained from HF/6-31G*, bond lengths (Å).

bond distances	$(EFPy)_n$				
	1	2	3	4	5
r(1,2)	1.386	1.386	1.386	1.388	1.386
r(2,3)	1.386	1.386	1.386	1.388	1.386
r(3,4)	1.390	1.390	1.390	1.390	1.390
r(4,5)	1.380	1.380	1.380	1.380	1.380
r(5,6)	1.390	1.390	1.390	1.390	1.390
r(6,1)	1.380	1.380	1.380	1.388	1.380
r(3,7)	1.472	1.472	1.470	1.467	1.470
r(7,12)	1.390	1.390	1.390	1.410	1.390
r(12,13)	1.520	1.520	1.520	1.520	1.520
r(13,4)	1.520	1.520	1.520	1.520	1.520
r(4,3)	1.390	1.390	1.390	1.410	1.390
r(7,8)	1.384	1.380	1.380	1.390	1.380
r(8,9)	1.384	1.380	1.380	1.390	1.380
r(9,10)	1.390	1.390	1.390	1.400	1.390
r(10,11)	1.390	1.390	1.390	1.410	1.390
r(11,12)	1.370	1.370	1.380	1.380	1.380
r(12,7)	1.390	1.390	1.390	1.410	1.390
r(10,14)	1.490	1.480	1.480	1.480	1.480
r(14,15)	1.320	1.320	1.320	1.350	1.320
r(15,16)	1.320	1.310	1.310	1.330	1.310
r(16,17)	1.380	1.390	1.390	1.400	1.390
r(17,18)	1.380	1.390	1.390	1.400	1.390
r(18,19)	1.380	1.380	1.380	1.380	1.370
r(19,14)	1.390	1.390	1.390	1.400	1.390

Table 4 Optimized angles and torsional angle of $(EFPy)_n$ (n = 1-5) as obtained from HF/ 6-31G*and angles (°).

angles	$(FPy)_n$				
	1	2	3	4	5
∠(3,7,12)	108.4	108.4	108.5	108.5	108.3
∠(7,12,13)	111.3	111.3	111.1	111.1	111.4
∠(12,13,4)	100.9	100.9	100.8	100.8	100.8
∠(13,4,3)	111.1	111.1	111.2	111.2	111.0
∠(4,3,7)	108.2	108.2	108.3	108.3	108.4
∠(7,8,9)	118.8	118.8	119.0	119.0	119.0
∠(8,9,10)	121.3	121.3	121.3	121.3	121.2
∠(9,10,11)	119.0	119.0	119.1	119.1	119.1
∠(10,11,12)	120.0	119.8	119.9	119.9	119.8
∠(11,12,7)	120.6	120.6	120.4	120.4	120.2
∠(12,7,8)	120.4	120.4	120.4	120.4	120.7
∠(14,19,18)	119.1	119.1	119.2	119.2	119.3
∠(19,18,17)	119.2	120.0	120.0	120.0	120.2
∠(18,17,16)	177.5	115.8	115.9	115.9	115.6
∠(17,16,15)	123.8	124.4	124.5	124.5	124.6
∠(16,15,14)	119.1	119.6	119.4	119.4	119.6
∠(15,14,19)	121.4	121.0	120.9	120.9	120.7
θ(11,10,14,15)	27.1	26.1	26.5	26.5	25.3

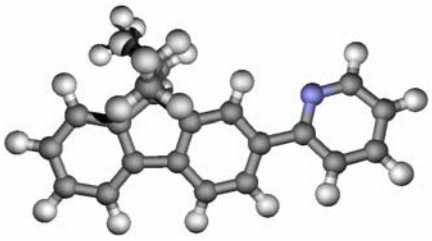

(a)

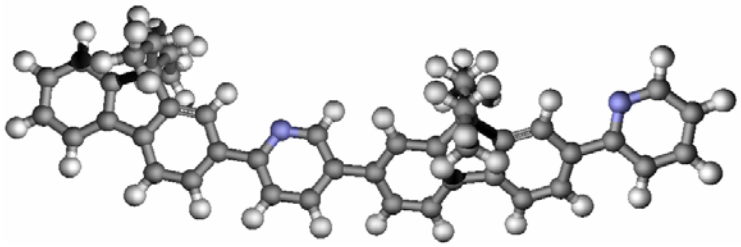

(b)

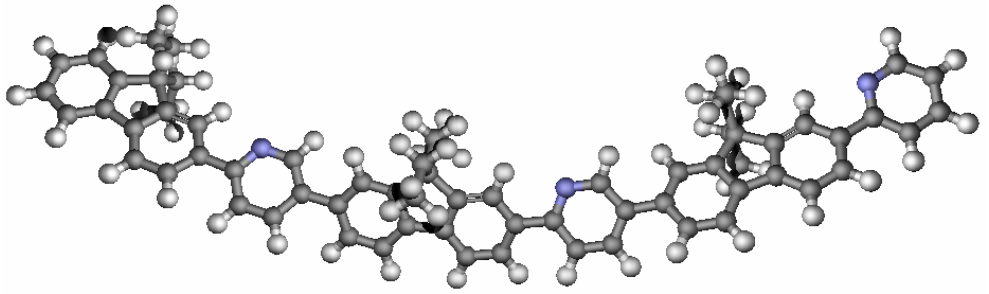

(c)

(e)

Figure 8 3D-structures of the $(EFy)_n$, n=1-4 calculated by HF/ 6-31G*.

3. Electronic Properties

3.1 HOMO-LUMO energy gaps

It is well-known that the energy gap of the polymer $(M)_n$ is the orbital energy difference between the highest occupied molecular orbital (HOMO) and the lowest unoccupied molecular orbital (LUMO) (Hay *et al.*, 2002, Curioni *et al.,* 2001, Hong *et al.,* 2001 and Wang *et al.,* 2004) when $n = \infty$. Nowadays, it is difficult to obtain the correct data by experiment due to the experimental condition limit, such as interchain interactions, solvent effects, and so on. The experimental energy gap is usually observed by two methods: the maximal wavelength in the spectra or the onset from CV-UV. They are valid when the lowest singlet excited state can be described by only one singly excited configuration in which an electron is promoted from HOMO to LUMO, and the experimental condition limit can be neglected (Wang *et al.*, 2004).

It has been proven that the density functional theory (DFT) method has successfully been used to study energy gap of conjugated organic polymers where the HOMO-LUMO energy differences provide a good estimate of the excitation energy (Kwon *et al.,* 2000). In this work, the HOMO-LUMO energy gaps ($\Delta_{H\text{-}L}$) were obtained from density functional theory (DFT) method as shown in Table 5-10. There is a good linear relation between the HOMO-LUMO energy gap and the inverse chain length (Figure 9-14). The extrapolated HOMO-LUMO energy gaps to the infinite chain length obtained from the plots were summarized in Table 11.

Form Table 11, one can see that the density functional theory with 6-31G*, 6-31G**, 6-31+G*, 6-31++G* and 6-311G* basis sets give corresponding values, except the 6-31G basis set. Therefore, the $\Delta_{H\text{-}L}$ calculated by the B3LYP/6-31G* method appears to be the sufficient method, as all higher basis sets give similar results. Moreover, the B3LYP/6-31G* is useful to calculate the HOMO-LUMO energy gaps of

EPFPy due to the less computational time than that of the various level of calculations. The extrapolated HOMO-LUMO energy gap obtained from B3LYP/6-31G* with the B3LYP/6-31G* optimized geometries gives a reasonable energy gap prediction as compared to the experimental data, 2.87 eV (Aubert *et al*, 2004). Their deviations are not more than 0.3 eV. It can be concluded that B3LYP/6-31G* is the approximated method to use in the investigation of $\Delta_{H\text{-}L}$ of this molecule.

Table 5 HOMO-LUMO energy gap of EFPy oligomers, calculated by B3LYP/ 6-31G//AM1, B3LYP/6-31G//HF/3-21G*, B3LYP/6-31G//HF/6-31G* and B3LYP/6-31G//B3LYP/6-31G* methods.

oligomers	HOMO-LUMO energy gap (eV)			
	B3LYP/6-31G //AM1	B3LYP/6-31G //HF/3-21G*	B3LYP/6-31G //HF/6-31G*	B3LYP/6-31G //B3LYP/6-31G*
n=2	3.93	4.02	4.09	3.76
n=3	3.75	3.87	3.92	3.58
n=4	3.68	3.81	3.86	3.50
n=5	3.64	3.78	3.81	3.45
n=∞	**3.43**	**3.61**	**3.62**	**3.24**

Table 6 HOMO-LUMO energy gap of EFPy oligomers, calculated by B3LYP/ 6-31G*//AM1, B3LYP/6-31G*//HF/3-21G*, B3LYP/6-31G*//HF/6-31G* and B3LYP/6-31G* methods.

oligomers	HOMO-LUMO energy gap (eV)			
	B3LYP/6-31G* //AM1	B3LYP/6-31G* //HF/3-21G*	B3LYP/6-31G* //HF/6-31G*	B3LYP/6-31G*
n=2	3.84	3.94	4.01	3.68
n=3	3.66	3.79	3.83	3.50
n=4	3.59	3.73	3.78	3.42
n=5	3.55	3.70	3.73	3.37
n=∞	**3.32**	**3.51**	**3.53**	**3.14**

Table 7 HOMO-LUMO energy gap of EFPy oligomers, calculated by B3LYP/ 6-31G**//AM1, B3LYP/6-31G**//HF/3-21G*, B3LYP/6-31G**//HF/6-31G* and B3LYP/6-31G**/B3LYP/6-31G* methods.

oligomers	HOMO-LUMO energy gap (eV)			
	B3LYP/6-31G** //AM1	B3LYP/6-31G** //HF/3-21G*	B3LYP/6-31G** //HF/6-31G*	B3LYP/6-31G** //B3LYP/6-31G*
n=2	3.84	3.94	4.01	3.68
n=3	3.66	3.79	3.83	3.50
n=4	3.59	3.72	3.77	3.42
n=5	3.55	3.69	3.73	3.37
n=∞	**3.35**	**3.52**	**3.54**	**3.16**

Table 8 HOMO-LUMO energy gap of EFPy oligomers, calculated by B3LYP/ 6-31+G*//AM1, B3LYP/6-31+G*//HF/3-21G*, B3LYP/6-31+G*//HF/ 6-31G* and B3LYP/6-31+G*//B3LYP/6-31G* methods.

oligomers	HOMO-LUMO energy gap (eV)			
	B3LYP/6-31+G* //AM1	B3LYP/6-31+G* //HF/3-21G*	B3LYP/6-31+G* //HF/6-31G*	B3LYP/6-31+G* //B3LYP/6-31G*
n=2	3.78	3.88	3.94	3.62
n=3	3.60	3.73	3.78	3.45
n=4	3.53	3.67	3.72	3.36
n=5	3.49	3.64	3.67	3.31
n=∞	**3.29**	**3.47**	**3.49**	**3.11**

Table 9 HOMO-LUMO energy gap of EFPy oligomers, calculated by B3LYP/ 6-31++G*//AM1,B3LYP/6-31++G*//HF/3-21G*,B3LYP/6-31++G*//HF/ 6-31G* and B3LYP/6-31++G*//B3LYP/6-31G* methods.

oligomers	HOMO-LUMO energy gap (eV)			
	B3LYP/6-31++G** //AM1	B3LYP/6-31++G** //HF/3-21G*	B3LYP/6-31++G** //HF/6-31G*	B3LYP/6-31++G** //B3LYP/6-31G*
n=2	3.78	3.88	3.94	3.62
n=3	3.60	3.73	3.78	3.45
n=4	3.53	3.67	3.72	3.36
n=5	3.49	3.64	3.67	3.31
n=∞	**3.29**	**3.47**	**3.49**	**3.11**

Table 10 HOMO-LUMO energy gap of EFPy oligomers, calculated by B3LYP/6-311G*//AM1, B3LYP/6-311G*//HF/3-21G*, B3LYP/6-311G*//HF/6-31G* and B3LYP/6-311G*/B3LYP/6-31G* methods.

oligomers	HOMO-LUMO energy gap (eV)			
	B3LYP/6-311G*//AM1	B3LYP/6-311G*//HF/3-21G*	B3LYP/6-311G*//HF/6-31G*	B3LYP/6-311G*//B3LYP/6-31G*
n=2	3.80	3.95	3.96	3.63
n=3	3.61	3.75	3.79	3.46
n=4	3.54	3.68	3.73	3.37
n=5	3.50	3.65	3.68	3.32
n=∞	**3.30**	**3.43**	**3.49**	**3.11**

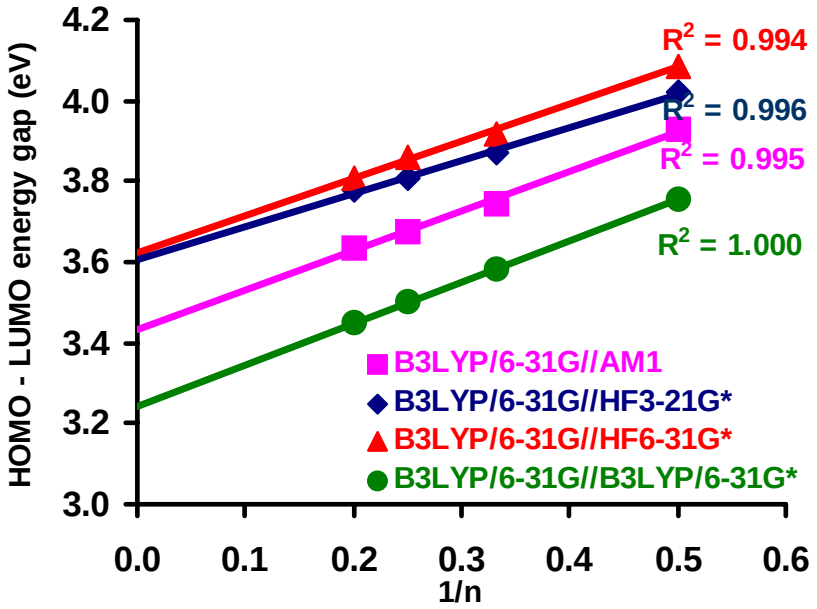

Figure 9 HOMO-LUMO energy gaps by B3LYP/6-31G as a function of reciprocal chain length *n* in oligomers of $(EFPy)_n$.

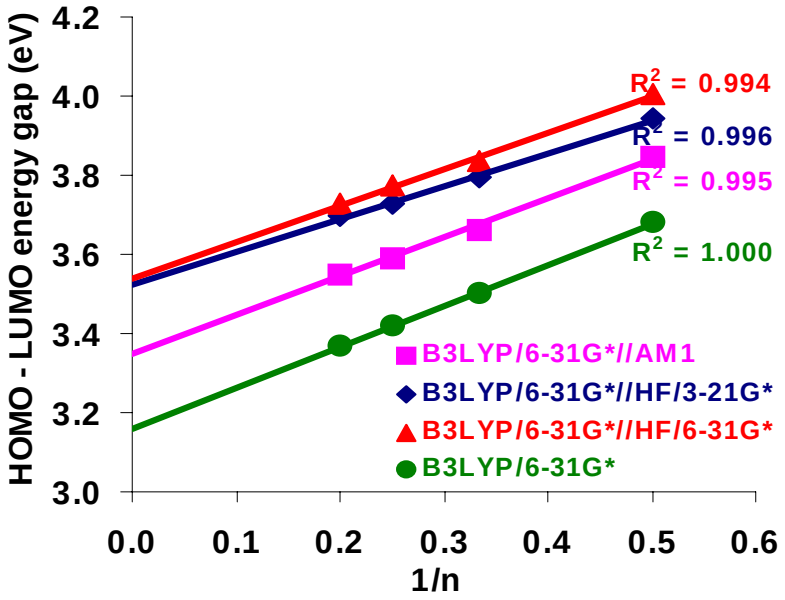

Figure 10 HOMO-LUMO energy gaps by B3LYP/6-31G* as a function of reciprocal chain length *n* in oligomers of $(EFPy)_n$.

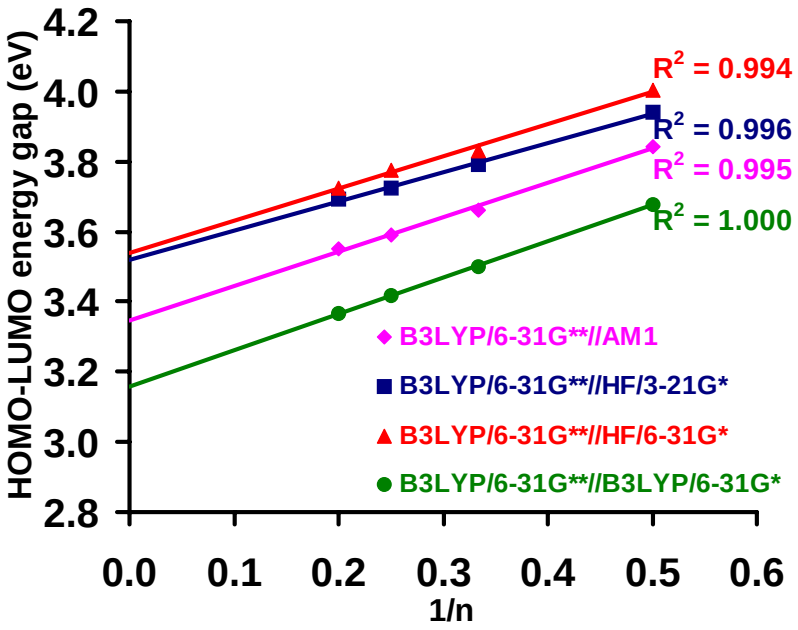

Figure 11 HOMO-LUMO energy gaps by B3LYP/6-31G** as a function of reciprocal chain length *n* in oligomers of $(EFPy)_n$.

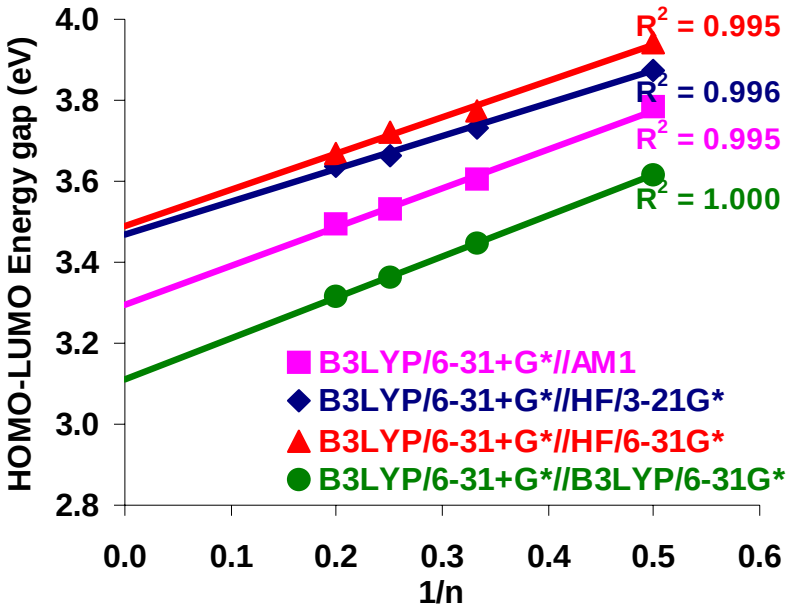

Figure 12 HOMO-LUMO energy gaps by B3LYP/6-31+G* as a function of reciprocal chain length *n* in oligomers of $(EFPy)_n$.

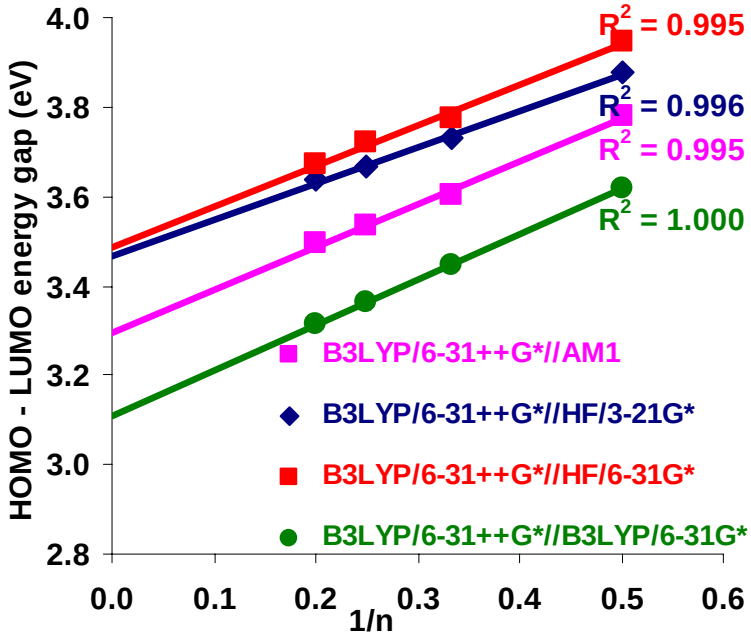

Figure 13 HOMO-LUMO energy gaps by B3LYP/6-31+G* as a function of reciprocal chain length *n* in oligomers of $(EFPy)_n$.

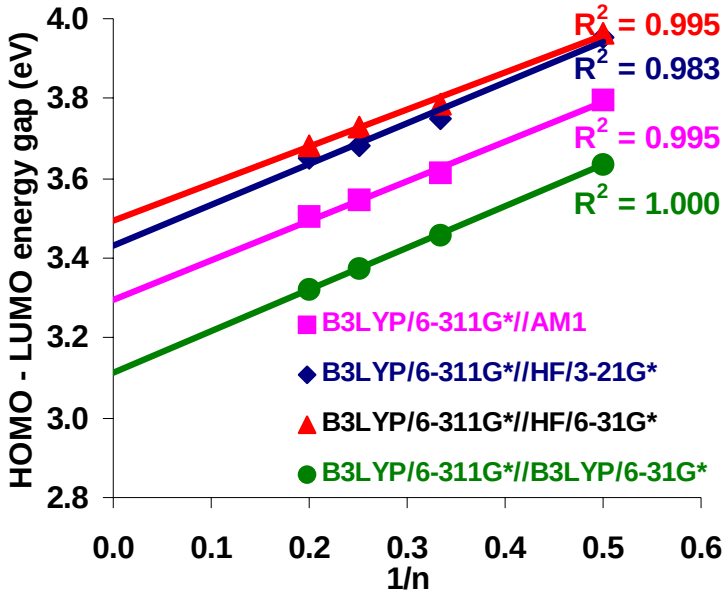

Figure 14 HOMO-LUMO energy gaps by B3LYP/6-311G* as a function of reciprocal chain length *n* in oligomers of $(EFPy)_n$.

It is desirable to obtain the useful information in the nature of the lowest singlet excited state by employing the HOMO-LUMO energy gap (Wang *et al.*, 2004). Because the HOMO-LUMO energy gap is easy to get, the approach can also be used to provide valuable information on estimate energy gaps of oligomers and polymers, especially treating even larger systems (Belletête *et al.*, 2000 and Wang *et al.* 2004). However, the orbital energy difference between HOMO and LUMO is still an approximate estimate to the transition energy since the transition energy also contains significant contributions from some two-electron integrals.

Table 11 Extrapolated HOMO-LUMO energy differences (Δ_{H-L}) of $(EFPy)_n$ calculated at various methods.

Methods	HOMO-LUMO energy differences (eV)
B3LYP/6-31G//AM1	3.43
B3LYP/6-31G//HF/3-21G*	3.61
B3LYP/6-31G//HF/6-31G*	3.62
B3LYP/6-31G//B3LYP/6-31G*	3.24
B3LYP/6-31G*//AM1	3.35
B3LYP/6-31G*//HF/3-21G*	3.52
B3LYP/6-31G*//HF/6-31G*	3.54
B3LYP/6-31G*	3.14
B3LYP/6-31G**//AM1	3.35
B3LYP/6-31G**//HF/3-21G*	3.52
B3LYP/6-31G**//HF/6-31G*	3.54
B3LYP/6-31G**//B3LYP/6-31G*	3.16
B3LYP/6-31+G*//AM1	3.29
B3LYP/6-31+G*//HF/3-21G*	3.47
B3LYP/6-31+G*//HF/6-31G*	3.49
B3LYP/6-31+G*//B3LYP/6-31G*	3.11
B3LYP/6-31++G*//AM1	3.29
B3LYP/6-31++G*//HF/3-21G*	3.47
B3LYP/6-31++G*//HF/6-31G*	3.49
B3LYP/6-31++G*//B3LYP/6-31G*	3.11
B3LYP/6-311G*//AM1	3.30
B3LYP/6-311G*//HF/3-21G*	3.43
B3LYP/6-311G*//HF/6-31G*	3.49
B3LYP/6-311G*//B3LYP/6-31G*	3.11
Expt.	**2.87**[a]

[a] Aubert *et al.*, (2004).

3.2 Excitation Energies

Due to an approximate estimate to the transition energy of orbital energy difference between HOMO and LUMO, therefore spectrum method was used to get some useful information for the experiment of the energy gap. The first 3 singlet-singlet electronic transitions of fluorene-pyridine oligomers were calculated with the ZINDO/S semi-empirical and TD-DFT levels of calculation. The excitation energies and oscillator strengths (*f*) from ZINDO/S and TD-B3LYP were illustrated in Table 12-15 and 16-19, respectively. All the cases of these studies, the electronic transitions with the large oscillator strength (>0.7) for the first singlet-singlet excitation ($S_0 \rightarrow S_1$ or $\pi \rightarrow \pi^*$) were obtained, implying a strong transition. Excitation to the S_1 state corresponds almost exclusively to the promotion of an electron from the HOMO to the LUMO, which are both delocalized over the whole molecule.

It will be useful to examine the highest occupied molecular orbital and the lowest virtual orbital for this oligomer to provide the framework for the excited state TD-B3LYP calculations in the subsequent section. The relative ordering of the occupied and virtual orbitals provides a reasonable qualitative indication of the excitation properties (DeOliveira *et al.,* 2000 and Wang *et al.,* 2005). The HOMO and LUMO orbitals of the EFPy monomer by B3LYP/6-31G* are depicted in Figure 15. The HOMO and LUMO of this molecule are localized predominantly on the phenyl rings, as shown in Figure 15. For these orbitals, there is antibonding between the bridge atoms and there is bonding between the bridge carbon atom and its conjoint atoms in the same benzenes in the HOMO. On the contrary, there are bonding in the bridge single bond and the antibonding between the bridge atom and its neighbor in the same phenyl ring in the LUMO.

Table 12 Electronic excitation energies (E_g), maximum absorption wavelengths (λ_{abs}) and oscillator strengths (*f*) for PEFPy oligomers calculated by ZINDO/S semiempirical at the AM1 optimized geometry.

n	$S_0 \rightarrow S_1$			$S_0 \rightarrow S_2$			$S_0 \rightarrow S_3$		
	E_g (eV)	λ_{abs} (nm)	*f*	E_g (eV)	λ_{abs} (nm)	*f*	E_g (eV)	λ_{abs}	λ_{abs} (nm)
1	3.83	323.9	0.83	4.14	299.7	0.01	4.28	289.5	0.03
2	3.51	353.7	2.04	3.84	323.1	0.07	4.07	304.7	0.02
3	3.40	364.6	3.11	3.64	340.9	0.18	3.84	323.1	0.33
4	3.36	369.1	3.95	3.52	352.1	0.63	3.70	335.4	0.16
5	3.33	371.9	4.85	3.46	358.7	0.79	3.59	345.0	0.39
∞	**3.20**	**384.1**							

Table 13 Electronic excitation energies (E_g), maximum absorption wavelengths (λ_{abs}) and oscillator strength (*f*) for PEFPy oligomers calculated by ZINDO/S semiempirical at the HF/3-21G* optimized geometry.

n	$S_0 \rightarrow S_1$			$S_0 \rightarrow S_2$			$S_0 \rightarrow S_3$		
	E_g (eV)	λ_{abs} (nm)	*f*	E_g (eV)	λ_{abs} (nm)	*f*	E_g (eV)	λ_{abs} (nm)	*f*
1	3.89	318.6	0.91	3.99	311.0	0.01	4.23	293.4	0.01
2	3.64	340.7	2.14	3.91	317.0	0.08	3.94	315.0	0.02
3	3.55	349.6	3.09	3.76	329.7	0.39	3.91	316.8	0.13
4	3.50	354.2	3.66	3.86	338.9	0.76	3.82	324.7	0.30
5	3.48	356.1	4.47	3.60	344.6	1.41	3.73	332.5	0.17
∞	**3.38**	**365.3**							

Table 14 Electronic excitation energies (E_g), maximum absorption wavelengths (λ_{abs}) and oscillator strength (*f*) for PEFPy oligomers calculated by ZINDO/S semiempirical at the HF/6-31G* optimized geometry.

n	$S_0 \rightarrow S_1$			$S_0 \rightarrow S_2$			$S_0 \rightarrow S_3$		
	E_g (eV)	λ_{abs} (nm)	*f*	E_g (eV)	λ_{abs} (nm)	*f*	E_g (eV)	λ_{abs} (nm)	*f*
1	3.96	313.5	0.87	4.16	298.1	0.01	4.24	292.3	0.01
2	3.68	337.0	2.10	3.97	312.5	0.09	4.11	301.6	0.02
3	3.58	346.2	3.10	3.80	325.9	0.31	3.97	312.2	0.16
4	3.54	350.1	3.94	3.70	335.4	0.67	3.86	320.9	0.28
5	3.51	353.3	4.42	3.63	341.6	1.43	3.76	329.7	0.23
∞	**3.40**	**362.5**							

Table 15 Electronic excitation energies (E_g), maximum absorption wavelengths (λ_{abs}) and oscillator strength (*f*) for PEFPy oligomers calculated by ZINDO/S semiempirical at the B3LYP/6-31G* optimized geometry.

n	$S_0 \rightarrow S_1$			$S_0 \rightarrow S_2$			$S_0 \rightarrow S_3$		
	E_g (eV)	λ_{abs} (nm)	*f*	E_g (eV)	λ_{abs} (nm)	*f*	E_g (eV)	λ_{abs} (nm)	*f*
1	3.78	327.8	0.93	4.13	299.9	0.01	4.18	296.6	0.01
2	3.44	360.5	2.18	3.78	327.9	0.10	4.09	303.5	0.01
3	3.34	371.4	3.16	3.59	345.1	0.39	3.79	326.9	0.16
4	3.28	377.5	3.95	3.47	357.7	0.79	3.66	338.9	0.30
5	3.25	391.2	4.42	3.39	366.0	1.68	3.54	350.1	0.12
∞	**3.13**	**398.7**							

Table 16 Electronic excitation energies (E_g), maximum absorption wavelengths (λ_{abs}) and oscillator strength (*f*) for PEFPy oligomers calculated by TD-B3LYP at the AM1 optimized geometry.

n	$S_0 \rightarrow S_1$			$S_0 \rightarrow S_2$			$S_0 \rightarrow S_3$		
	E_g (eV)	λ_{abs} (nm)	*f*	E_g (eV)	λ_{abs} (nm)	*f*	E_g (eV)	λ_{abs} (nm)	*f*
1	4.03	307.8	0.71	4.49	276.0	0.01	4.56	272.1	0.02
2	3.44	360.7	1.84	3.88	319.9	0.06	4.02	308.5	0.04
3	3.24	382.1	2.87	3.60	344.5	0.13	3.68	337.4	0.09
4	3.18	390.2	3.68	3.42	362.9	0.48	3.55	349.4	0.15
5	3.13	395.6	4.63	3.31	374.4	0.61	3.49	355.0	0.15
∞	**2.89**	**417.6**							

Table 17 Electronic excitation energies (E_g), maximum absorption wavelengths (λ_{abs}) and oscillator strength (*f*) for PEFPy oligomers calculated by TD-B3LYP at the HF/3-21G* optimized geometry.

n	$S_0 \rightarrow S_1$			$S_0 \rightarrow S_2$			$S_0 \rightarrow S_3$		
	E_g (eV)	λ_{abs} (nm)	*f*	E_g (eV)	λ_{abs} (nm)	*f*	E_g (eV)	λ_{abs} (nm)	*f*
1	4.04	306.6	0.78	4.43	280.1	0.00	4.48	277.0	0.02
2	3.54	350.1	1.85	3.96	312.8	0.06	4.06	305.8	0.06
3	3.38	366.3	2.78	3.71	334.6	0.25	3.78	327.9	0.11
4	3.31	374.2	3.59	3.54	350.1	0.55	3.67	337.5	0.13
5	3.28	378.0	4.23	3.45	359.7	1.14	3.63	341.7	0.22
∞	**3.07**	**395.9**							

Table 18 Electronic excitation energies (E_g), maximum absorption wavelengths (λ_{abs}) and oscillator strength (*f*) for PEFPy oligomers calculated by TD-B3LYP at the HF/6-31G* optimized geometry.

n	$S_0 \rightarrow S_1$			$S_0 \rightarrow S_2$			$S_0 \rightarrow S_3$		
	E_g (eV)	λ_{abs} (nm)	*f*	E_g (eV)	λ_{abs} (nm)	*f*	E_g (eV)	λ_{abs} (nm)	*f*
1	4.13	300.5	0.76	4.53	273.8	0.01	4.61	268.9	0.01
2	3.60	344.7	1.83	4.01	309.0	0.07	4.14	299.8	0.06
3	3.42	362.9	2.81	3.75	330.6	0.21	3.83	323.4	0.12
4	3.36	369.2	3.65	3.58	346.4	0.50	3.73	332.8	0.14
5	3.31	374.8	4.19	3.48	356.4	1.13	3.66	338.5	0.21
∞	**3.09**	**392.7**							

Table 19 Electronic excitation energies (E_g), maximum absorption wavelengths (λ_{abs}) and oscillator strength (*f*) for PEFPy oligomers calculated by TD-B3LYP at the B3LYP/6-31G* optimized geometry.

n	$S_0 \rightarrow S_1$			$S_0 \rightarrow S_2$			$S_0 \rightarrow S_3$		
	E_g (eV)	λ_{abs} (nm)	*f*	E_g (eV)	λ_{abs} (nm)	*f*	E_g (eV)	λ_{abs} (nm)	*f*
1	3.93	315.2	0.80	4.38	282.9	0.02	4.49	276.0	0.00
2	3.30	375.8	1.96	3.77	328.8	0.06	3.90	318.0	0.07
3	3.11	398.9	2.92	3.49	355.4	0.23	3.54	350.0	0.15
4	3.02	410.4	3.72	3.29	376.4	0.59	3.40	364.6	0.13
5	2.97	417.6	4.24	3.17	391.4	1.35	3.32	373.0	0.11
∞	**2.71**	**441.7**							

The lowest excitation energies, E_g calculated by ZINDO and TD-DFT as a function of reciprocal chain length n in PEFPy were presented in Figure 16 and 17, respectively. Good linear relationship was found between the calculated excitation energy by ZINDO/S and TD-DFT methods and the reciprocal chain length n in the oligomers of PEFPy.

The lowest excitation energies of PEFPy calculated with ZINDO/S and TD-DFT were summarized in Table 20. One can see that, the TD-DFT method is better compared to ZINDO/S in meeting the experimental data. From Table 20, TD-DFT//B3LYP/ 6-31G* predictions systematically underestimate the energy gaps due to the nature of method. However, the small error was responsible from three factors: one is that calculations in a few longer oligomers may be required so that more data could be used in linear regression. Another is that the predicted energy gaps are for isolated gas-phase chains, while experimental energy gaps are measured in the condensed phase where interchain interactions may be significant. Additionally, the methods of calculation and experiment have fault in themselves. Consequently, TD-B3LYP//AM1 exhibits a better agreement with experimental observation. On the other hand, the TD-DFT//HF3-21G* and TD-DFT//HF6-31G* calculations provided a relatively large energy gap of 3.10 and 3.11 eV respectively which are broader than the experimental values.

EFPy

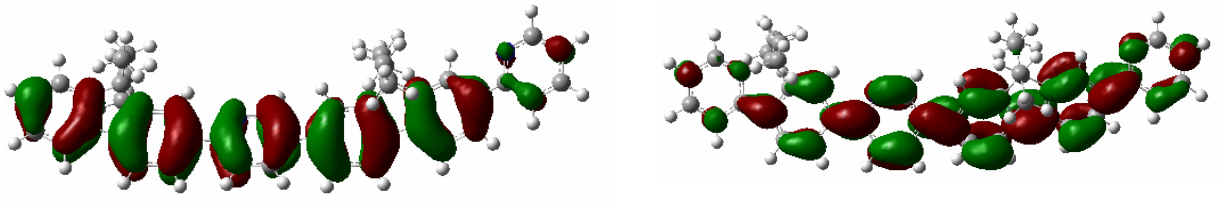

$(EFPy)_2$

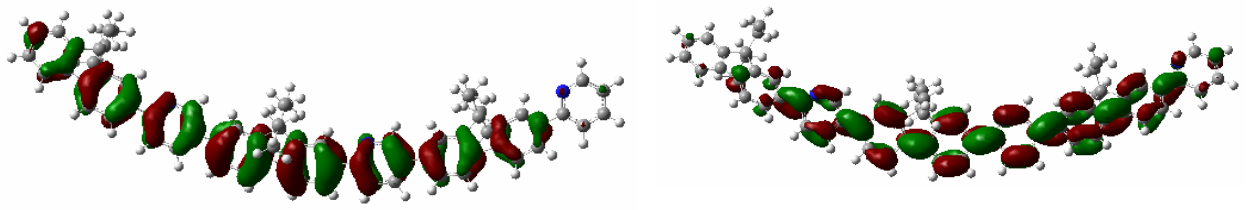

$(EFPy)_3$

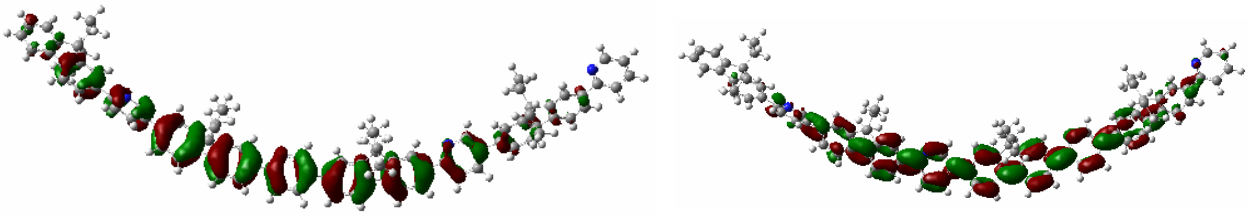

$(EFPy)_4$

HOMO **LUMO**

Figure 15 HOMO and LUMO orbitals of the $(EFy)_n$, n=1-4 calculated by B3LYP/ 6-31G*.

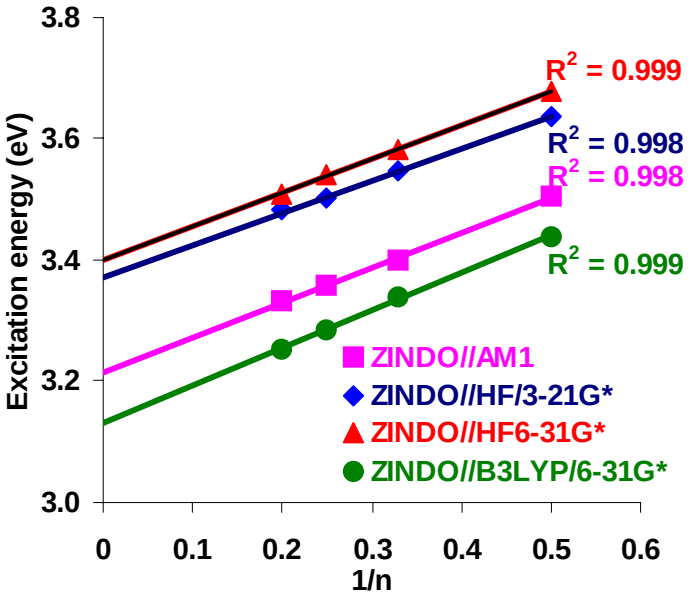

Figure 16 Excitation gaps of PEFPy extrapolated from the plot of excitation energies of the oligomers versus the inverse number of monomer units as obtained from ZINDO/S.

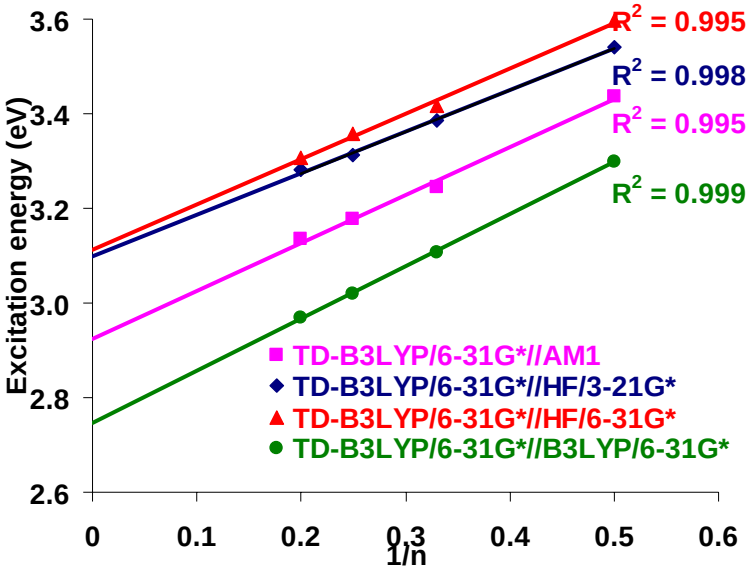

Figure 17 Excitation gaps of PEFPy extrapolated from the plot of excitation energies of the oligomers versus the inverse number of monomer units as obtained from TD-B3LYP.

Table 20 Extrapolated energy gaps of PEFPy calculated at various methods.

method	E_g (eV)
ZINDO//AM1	3.20
ZINDO//HF/3-21G*	3.38
ZINDO//HF/6-31G*	3.40
ZINDO//B3LYP/6-31G*	3.13
TD- B3LYP/6-31G*//AM1	2.89
TD- B3LYP/6-31G*//HF/3-21G*	3.07
TD- B3LYP/6-31G*//HF/6-31G*	3.09
TD- B3LYP/6-31G*//B3LYP/6-31G*	2.75
Expt.[a]	3.20 (thin film) 3.26(THF solution)

[a] Aubert *et al*, (2004).

3.3 Absorption wavelength

ZINDO/S and TD-B3LYP methods were used on the basis of optimized geometry (AM1, HF/3-21G*, HF/6-31G* and B3LYP/6-31G*) to obtain the nature and energy of the singlet-singlet electronic transitions of EFPy in all series under study. In this study, the excitation energies, oscillator strengths and maximum absorption wavelengths obtained by ZINDO/S and TD-B3LYP calculations for the most relevant first three singlet excited state in $(EFPy)_n$.

As shown in Table 12-19, all electronic transition are of the $\pi\pi^*$ type and involve both subunits of the molecule. In other words, no localized electronic transitions are calculated among the first three singlet-singlet transitions. Both methods show the

excitation to the S_1 state corresponds almost exclusively to the promotion of an electron from the HOMO to the LUMO. The oscillator strengths of the $S_0 \rightarrow S_1$ electronic transition are larger in each oligomer. The oscillator strength associated with the S_1 state increases by about 1 order of magnitude upon adding one repeated unit to the monomers in all series.

Obviously, the strongest absorption peaks are assigned to ππ* electronic transition character arising exclusively from $S_0 \rightarrow S_1$ electronic transition composed mainly of the HOMO → LUMO transition. From Tables 12-19, the absorption wavelengths increase with the conjugation lengths increasing, as in the case of oscillator strength. This is reasonable because the HOMO-LUMO transition predominant in the $S_0 \rightarrow S_1$ electronic transition, as the analyses above show, with the extension of molecular size, the HOMO-LUMO energy gaps decrease.

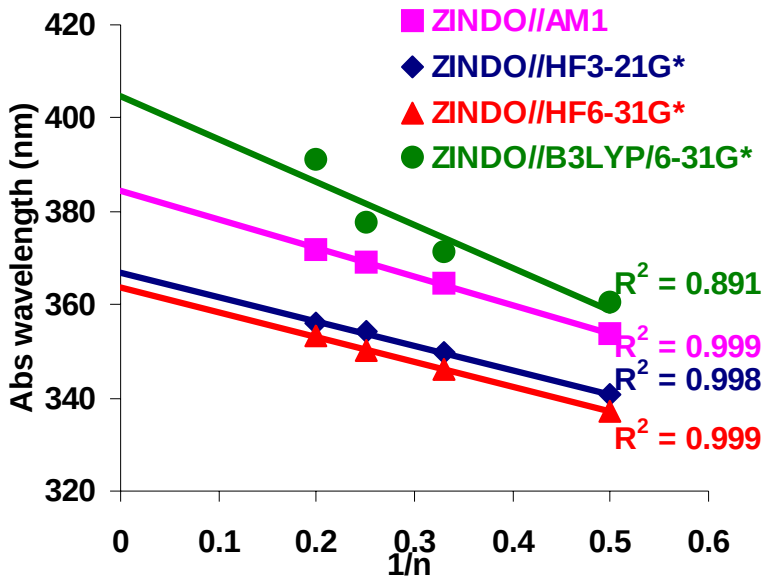

Figure 18 Plots of absorption wavelength of the $(EFPy)_n$ versus the inverse number of chain length obtained from ZINDO.

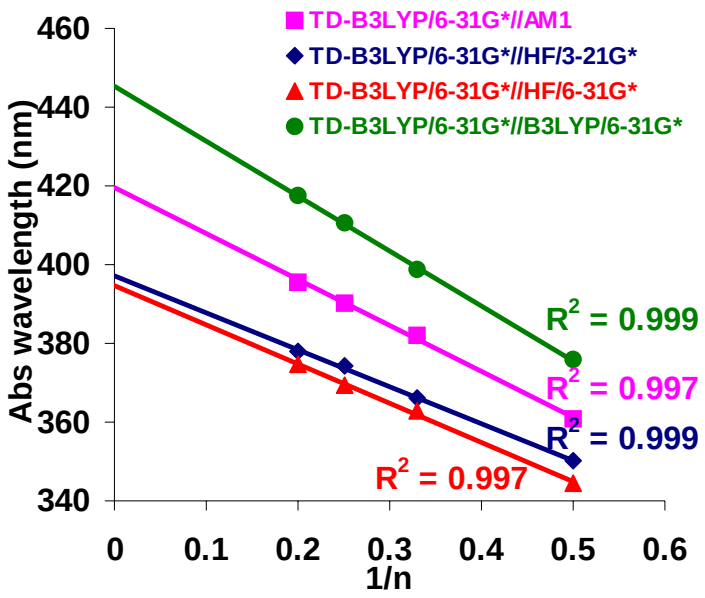

Figure 19 Plots of absorption wavelength of the $(EFPy)_n$ versus the inverse number of chain length obtained from TD-B3LYP.

Table 21 Extrapolated absorption wavelengths of PEFPy calculated at various methods.

Methods of calculation	λ_{abs} (nm)
ZINDO//AM1	384.1
ZINDO//HF/3-21G*	365.3
ZINDO//HF/6-31G*	362.5
ZINDO//B3LYP/6-31G*	398.7
TD- B3LYP/6-31G*//AM1	417.6
TD- B3LYP/6-31G*//HF/3-21G*	395.9
TD- B3LYP/6-31G*//HF/6-31G*	392.7
TD- B3LYP/6-31G*//B3LYP/6-31G*	441.7
Expt.	380[a], 388[b]

[a] the data was measured in solution (Aubert *et al.*, 2004)

[b] the data was measured in film (Aubert *et al.*, 2004)

Figure 18 and 19 show the plots of absorption wavelength of the $(EFPy)_n$ versus the inverse number of chain length obtained from ZINDO and TD-B3LYP, respectively. All plots show excellent linearity, however, absorption wavelengths of ZINDO//AM1 deviate somewhat from linearity. This deviation was traced to a dramatic decrease of the ring torsional angles from the dimer to pentamer. The extrapolated absorption wavelengths were listed in Table 21. It was found that TD-B3LYP calculations overestimate the absorption wavelength compared to ZINDO results and the experimental data. Many investigations show that TD-B3LYP is a good tool for predicting the absorption spectra of molecules. However, this method has defects when studying extended systems. Frequently, the optical properties reach saturation quickly for short chain lengths, whereas the orbital energies continue to change for longer oligomers. It is know that the exchange-correlation (XC) functionals must decrease with the decreasing chain lengths. This trend of variation is in line with expectation that in more extended systems the electronic repulsion is smaller. However, because atomic structures of molecules are alike and are calculated with the same methods and basis sets, the results can still reflect some variation trend (Yang *et al.*, 2005).

4. Excited State Geometries

Up to now, the standard method in Gaussian03 for calculating excited state equilibrium properties of larger molecules is the configuration interaction singles (CIS) method. However, because of the neglect of electron correlation, CIS results are not accurate enough in many applications. In this Gaussian study, I hope to investigate the excited-state properties by this method despite the fact that they may not be accurate. Because the calculation of excited state properties typically requires significantly more computational effort than is needed for the ground states and is dramatically constrained by the size of the molecules (Yang *et al*., 2005 and 2006).

In this study, the excited state of FPy monomer was calculated using CIS/3-21G* and CIS/6-31G*. The excited state structures were compared to their ground state structures calculated by HF/3-21G* and HF/6-31G*. The distances and the torsional angle of FPy excited state geometry were summarized in Table 22.

Table 22 The optimized bond distances and torsional angle calculated by using HF/ 3-21G*, HF/6-31G*, CIS/3-21G* and CIS/6-31G*.

	Ground state		Excited state	
Bond length (Å)	HF/3-21G*	HF/6-31G*	CIS/3-21G*	CIS/6-31G*
C1-C2	1.387	1.386	1.372	1.372
C2-C3	1.387	1.386	1.412	1.415
C3-C4	1.390	1.390	1.429	1.425
C4-C5	1.370	1.380	1.370	1.375
C5-C6	1.390	1.390	1.394	1.394
C6-C1	1.380	1.380	1.400	1.402
C7-C8	1.380	1.384	1.422	1.424
C8-C9	1.380	1.384	1.356	1.357
C9-C10	1.390	1.390	1.442	1.443
C10-C11	1.390	1.390	1.434	1.435
C11-C12	1.370	1.370	1.350	1.355
C12-C7	1.390	1.390	1.443	1.437
C10-C14	1.480	1.490	1.427	1.435
C14-N15	1.330	1.320	1.364	1.355
N15-C16	1.320	1.320	1.313	1.305
C16-C17	1.380	1.380	1.392	1.394
C17-C18	1.380	1.380	1.389	1.388
C18-C19	1.380	1.380	1.374	1.375
C19-C14	1.390	1.390	1.414	1.417

Torsion (^{o})	HF/3-21G*	HF/6-31G*	CIS/3-21G*	CIS/6-31G*
C9-C10C-14-C19	-11.5	-28.5	0.0	0.0

It was found that the changes in basis set of the ground state lead to a slightly difference in geometry parameters. As can be seen from Table 22, there are a number of structural differences between the ground state and excited state geometries. The bond lengths, C_1-C_2, C_4-C_5, C_8-C_9, C_{11}-C_{12}, C_{10}-C_{14}, C_{18}-C_{19} and C_{15}-C_{16} become shorter in excited state. On the other hand, the bonds closed to them become a bit longer. These clearly indicate that the monomers are becoming more quinoid like in the excited state. It is obvious that the excited structure has a strong coplanar tendency, that is, the conjugation is better in excited state.

From Figure 15, the results show that there are differences in bond distances between the ground state (S_0) and lowest singlet excited state (S_1) from molecular orbital nodal patterns. Because the lowest singlet state corresponds to an excitation from the HOMO to the LUMO in all of the considered oligomers, the bond distances variation by analyzing the HOMO and LUMO were explored.